Effect Of Changing Landuse on Surface Temperature in Some Parts of Kano Metropolis, Kano-Nigeria

Abubakar Nuhu[1] Abdulmalik A Yakubu[2] Oyibo Abubakar Sadiq[3] Abubakar Adamu[4] Isah Alhaji Isah[5], Atoku Ibrahim Aminu[6,] Yakubu Men Daniel[7], Itiveh Samson Elo[8]

[1,2,3,4,6,7,8] *Space Application Department, Zonal Advanced Space Technology Applications Laboratory, Kano*

[5] *Space Exploration Department, Zonal Advanced Space Technology Applications Laboratory, Kano*

Abstract*—Remote sensing and GIS play an important role in monitoring the land use and land cover changes and land surface temperature. In recent years, researchers have conducted many researches on the impact of land use and land cover on land surface temperature (LST). In this study, the impact of land use and land cover on LST in part of Kano metropolis was analyzed using geospatial techniques. Landsat image of 2000, 2010 and 2020 were used for supervised classification using maximum likelihood in ArcGIS 10.3.1. Four classes were identified, namely; vegetation, farmland, built up area and bare land. In the computation of LST thermal bands from the images were used to extract LST. To establish the relationship between land use dynamics and LST, NDVI, NDBI and NDWI were also computed and used as input data. Relationship between LULC and LST was realized and the finding from the research revealed that, bare land and built-up area exhibited more surface temperature than farmland and vegetation in 2000, 2010 and 2020 year. In 2000 it shows that built-up area exhibited temperature value that ranging from 28.6℃ to 31.4℃, and bareland with the value from 27.8 to 28.5 to 2 .5℃ to 26.8℃ 26.9 to 27.7, respectively. While in 2020, bare land and built-up area exhibited more surface temperature with values ranging o 35.5℃ to 47.4℃ 33.8℃ to 35.4℃, V to 24.5℃ to 31.6℃ 31.7℃ to 33.7℃. Therefore, the result indicated a positive correlation between NDBI and LST and negative correlation between NDVI and LST in the study area. Implication of LST in the study area such as high effect to the older once because majority of them are into farming which explain how exposed they are to heat.

***Index Terms*—LST, NDVI, NDBI, UHI, LULC.**

I. INTRODUCTION

Urban Heat Island (UHI) is a phenomenon that results from increased temperature thus affecting millions of people worldwide [1]. Higher temperatures are experienced mostly in urban areas when compared to the surrounding countryside, is reported to have enormous consequences on the health and wellbeing of people living in these cities [2].

As urban areas of the world develop, changes occur in their landscape, buildings, roads, and other infrastructural facilities, which replace open spaces and vegetation. Surfaces that were once permeable and moist have become impermeable and dry [3]. These changes continue to cause urban regions to become warmer than their out skirts or rural surroundings or fringes, forming an “Island” of higher temperatures in the landscape [4]. Heat islands occur on the surface and in the atmosphere; surface urban heat islands are typically present day and night but tend to be strongest during the day when the sun is shining [4]. In contrast, the atmospheric urban islands are often weak during the late morning and throughout the day and become more pronounced after sunset due to a slow release of heat from infrastructures such as building materials, road materials and pavement materials etc [3].

Kano state and its environs have experienced rapid development and high growth of urbanization and industrialization over the past two decades. These urban transfusions, especially in Dawakin Tofa and Ungogo conurbation, have altered its physical and natural environment [5]. Urban encroachment is significant especially in urbanized districts like Dawanau in Dawakin Tofa, transferred rural environment into a new urban landscape. Overtime, a largely rural area of agricultural land has been converted into urban areas, hence changed the

surface profile of the area. The urban surfaces absorb heat and increase the temperature comparatively to the surrounding area. The heat bubble, known as urban heat island (UHI) not only reduced human comfort ability but it also could increase energy consumption in buildings ([6] and [7]).

One of the common features of Kano City, which is the second largest industrial center and largest commercial state in Nigeria, is rapid development and population growth rate, the population of the metropolis at (the year 2000) is 1.6million [8] and it is projected to be 3.6million in 2014 [9] Kano records high rate of immigrants into the state for different reasons including business and leisure, which has been increasing at 30 to 40 per cent per annum [10].As a result of this, more infrastructure needs to be put in place to accommodate its ever increasing population, and as more vegetative cover are being cleared to cover up for the infrastructure of the increasing population, this tends to lead to urban heat island. According to the UN, 2018 report that populated countries such as China, India, and Nigeria, are likely to occupy 35% of the global urban population growth between 2018 and 2050. UHI, therefore, has gained considerable research interest and has been the subject of active investigation, especially in the last decade.

Though [11] worked on Spatial and Temporal Changes of Urban Heat Island in Kano Metropolis, Nigeria clearly showed the presence of urban heat island in Kano metropolis. The study did not analyze the annual time-series. The study also did not precisely determine the level of the change in land surface temperature and Normalized Different Vegetation Index (NDVI) in at a shorter interval in the study area, which is the gap this study intends to address using the interval of one year.

This study is directly aimed at conducting an annual time-series evaluation of land surface temperature using Landsat thermal image, The study intends to examine the spatial and temporal variations and patterns of land surface temperature (LST) in the context of normalized difference vegetation index (NDVI) and land use/land cover (LULC) in some parts of Kano metropolis, Nigeria. Landsat 2000 – 2020 respectively will be used for this analysis. The various analysis involved in this study were land use land cover analysis and change estimation, land surface temperature estimation and normalized difference vegetation index analysis.

II. STUDY AREA

Kano state extends from latitudes 10˚3′ N to 12˚ 30′ N and longitude 7˚35′ E to 9˚20′ E (Figure 1.0). It is made up of 44 Local Government Areas. Out of which 38 are in the rural areas of the state. The total land area of the state is about 20,760sq km [12]. The total population in the 2006 national census is about 9,386,820 people [9]. The study area, Kano metropolis lies between latitude 11˚05′ to 12˚07′ N and longitude 8˚22′ to 8˚47′ E and altitude 472 meters above sea level. Kano Metropolis bordered by Minjibir LGA to the Northeast and Gezawa LGA to the East, Dawakin Kudu LGA to the South East and Madobi and Tofa LGAs to the South West [13].

The study area includes three metropolitan local government of Kano State namely Dala Local Government, Fagge Local Government, and Kano Municipal Local Government.

According to historical sources, Kano city was founded around Dala Hill in the 9th century [14]. [14] is of the view that the spatial planning and development of the area started with the building of the first city wall between 1095 and 1134, which started east of the Kurmi market near the Jakara stream. After independence, Kano witnessed unprecedented urbanization and rapid population growth due to socio-economic transformation in the state. According to [15] as cited in [16], by the time colonial masters came in early 20th century, what constitutes Kano and virtually encompassed by the wall was contained within 17.5 km^2. Today metropolitan Kano (made up of the declared urban area in accordance with the Land Use and Allocation Committee) is contained within 60 km^2, while the built-up metropolitan Kano is contained within 40 km^2 [14].

GFigure 1.0: Location map of the Study area-Kano metropolis, Nigeria.

III. MATERIALS AND METHODOLOGY

A. Data Used

The selection of appropriate spatial and temporal image is an essential step to investigate any changes and consequently, to analyze them. Remotely sensed

multi-temporal Landsat data series (Table 1 below) will serve as the primary data source, it spans from 2000 - 2020 with a (1year interval). Secondary data will include administrative and topographic maps and satellite image.

Multi sensor satellite data such as Landsat 8 of different years of both the wet and dry season have been acquired from the USGS website as the same sensor data is not available over the chosen study period. Imageries of both the wet and dry season were used to limit the effect of seasonal variation error, i.e., to limit to influence of climatic conditions on the vegetation and of the land surface temperature respectively. Different scenes of imagery were acquired because the study area cuts across different scenes of Landsat global coverage.

B. Software's used in the study include

Software's use for image pre-processing, image processing, image analysis and result generation and presentation include ESRI ArcGIS version 10.5**,** Idrisi Selva**,** Microsoft office 2016 and Microsoft Excel 2016.

TABLE 1 CHARACTERISTICS OF IMAGES AND THE SENSOR USE IN CAPTURING THESE IMAGES

Satellite Sensors/Imagery Characteristics	Landsat 8 (OLI & TIRS)	Landsat 7 Enhanced Thematic Mapper (ETM+)
Platform	Landsat8 (Launched October 2013)	Landsat 7 (Launched Aril 15, 1999)
Orbit	16 day/705 km	16days
Equatorial crossing time	10:00 am	10:00 am
Swath width	185km	
Bands	1 (0.45-0.52µm) 2 (0.52-0.60µm) 3 (0.63-0.69µm) 4 (0.76-0.90µm) 5 (1.55-1.75µm) 6 (10.4-12.5µm) 7 (2.08-2.35µm) panchromatic band 8 (0.50-0.90µm)	1 (0.45-0.52µm) 2 (0.52-0.60µm) 3 (0.63-0.69µm) 4 (0.77-0.90µm) 5 (1.55-1.75µm) 6 (10.4-12.50µm) 7 (2.08-2.35µm) 8 (0.52-0.90µm)
Spatial resolution	28.5	
Radiometric resolution	16 bits	
Date of Image acquisition	2000-2010	2010-2020
Path and row	188/052 188/052 188/052	188/052 188/052 188/052
Coverage Issues	Less than 10 per cent cloud cover	
Pre-processing history	L1T (terrain corrected)	

The method adopted for this study to model the land surface temperature of Kano municipal, Dala, Gwale and its environs is given below (Figure 2).

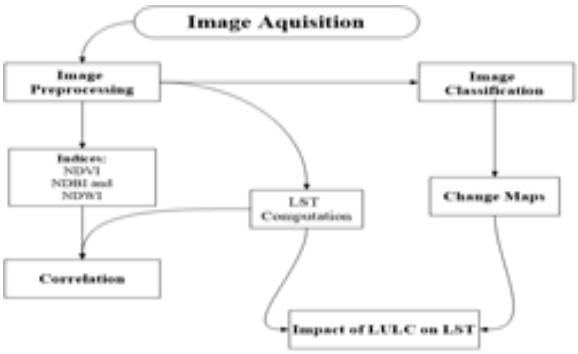

Figure 2: Methodology Flow Chart for the Study

The different scenes of the different years of the Landsat series considered for the study were mosaicked together to combine the different raster datasets into a new seamless raster dataset, this was accompanied with the aid of Idrisi Selva software. This was followed by sub-setting the area of interest of each band from the new-mosaicked raster dataset.

Before the processing and analysis of the image data occurred, various pre-processing routines, appropriate to the desired output, was applied to the imagery. These enhance the quality of the image data by reducing or eliminating various radiometric and geometric errors caused by internal and external conditions. Geometric correction procedures address errors in the relative position of pixels due to factors such as variation in altitude, attitude and velocity of the sensor platform, Earth curvature, panoramic distortion, relief displacement and non-linearities in the sweep of a sensor [17].

C. Data pre-processing

Absorption and scattering create an overall effect of "haziness" which reduces the contrast in the image. Scattering also creates the "adjacency effect" in which the radiance recorded for a given pixel partly incorporates the scattered radiance from neighboring pixels. In order to make a meaningful measure of radiance at the Earth's surface, the atmospheric interferences must be removed from the data. This process is called "atmospheric correction" [18].

The first step in the process of atmospheric correction is the removal of atmospheric effects due to absorption and scattering which is the major contributing factor to the haziness of an image. To correct for this, the images were rectified for path radiance using Dark Object Subtraction (DOS) method [19], this method was chosen for its simplicity and rapidity. While applying this method, the pixel having minimum brightness value in each band of each image was detected and that value was subtracted from the pixel values in the corresponding band. This resulted in the atmospherically corrected images. The equation used for dark object subtraction (DOS) is given below:

DOS = DN's of image – DN of minimum brightness in the image (i)

After the radiometric correction, a geometric correction was done on all the images. Accurate geometric corrections and referencing are the indispensable prerequisites to perform change detection analyses. Without this, the results will lose its reliability, and analyses would fail to diagnose changes accurately [18]. No additional measure was applied to further rectify the image. All the images were projected in Universal Transverse Mercator (UTM) projection (WGS 84, zone: 32 North), this coordinate system was obtained throughout the project [18].

D. Land use/ Land cover Classification

The land cover classification of the study area will be done using the Idrisi software. A supervised pixel-based image classification technique was employed in carrying out the study. The type of classification used here is the maximum likelihood classification; an extensive classification algorithm that touches a probability density function, meaning the classifier guesses the probability with which a specific pixel belongs to a specific class. Band combination 5, 4, 3 of Landsat 8 (OLI/TIRS) image of the study area were chosen for further classification analysis because it gives the false colour composite of the image and thereby gives the maximum information for land cover classification.

Maximum likelihood method of the classification algorithm is one of the common parametric classifiers used for supervised classification. The algorithm is used for Computing the weighted distance or likelihood (D) of unknown measurement vector (X) belonging to one of the known classes (Mc) which are based on the Bayesian equation.

$$D = \ln(a_c)-[0.5\ln(cov_c)]-[0.5(X-M_c)\ T(cov_c-1)\ (X-M_c)] \quad \text{(ii)}$$

By using pixel-based classification method such as the maximum likelihood classifier, the LULC map for the years 2014, 2015, 2016, 2017 and 2018. [20] stated that pixel-based classification method extracts information from images based on pixels, which rely on prior knowledge of the diverse land classes in the image, which can be known through field surveys, or from any form of existing source of information. The knowledge of these features will be used to select training pixels for classification into five different land cover classes, which are built-up /roads, grassland, vegetation, water body, riparian and bareland.

Calculations of LULC indices

The LULC indices such as NDBI, NDWI and NDVI) will be estimated using the Red, Green, NIR, and SWIR bands. The indices will be utilized to establish a relationship with LST. Equations 1, 2, and 3 shows the equations used for the calculation of indices.

$$NDVI = \frac{NIR-RED}{NIR+RED} \quad [21] \quad \text{(iii)}$$

$$NDWI = \frac{GREEN-NIR}{GREEN+NIR} \quad [22] \quad \text{(iv)}$$

$$NDBI = \frac{SWIR-NIR}{SWIR+NIR} \quad [23] \quad \text{(v)}$$

E. Computation of Land Surface Temperature

Surface Temperature is one of the significant variables that have been measured by remote sensing satellites. This information has a variety of usages in environmental and ecological studies as well as for spatial decision making in GIS.

To obtain actual surface temperature information,

a) The DNs was converted to top of-the-atmosphere (ToA) radiance values, and then.
b) The ToA radiance values will be converted to ToA brightness temperature in Kelvin.

Mathematically;

The DNs were converted first to satellite radiance using the following equation:

$$L\lambda(LANDSAT\ 7TM) = Lmin + \frac{lmax-lmin}{Qcal_{max}+Qcal_{min}} \times DN \quad \text{(vi)}$$

$$LST = \frac{T_B}{1+\left(\lambda \times \frac{T_B}{\rho}\right)*\ln(\varepsilon)} - 273.15 \quad \text{(vii)}$$

$$\rho = \frac{h \times c}{\alpha} = 1.438 \times 10 - 2mK \quad \text{(viii)}$$

$$T_B = \frac{K_2}{\ln\left(\frac{K_1}{L\lambda}+1\right)} \quad \text{(ix)}$$

Equation one can also be expressed as;

$L\lambda = LMIN + (LMAX-LMIN) \times DN/255$ (x)

Where:

$L\lambda$ = Spectral Radiance,

QCAL = the quantized calibrated pixel in DN,

LMIN = Spectral Radiance of DN value 0,

LMAX = Spectral Radiance of DN value 255.

The spectral radiance values were transformed to radiant surface temperature values in kelvin using the following equation:

$Tb = k2/(In(k1/L\lambda + 1)$ (xi)

Tb = Surface Temperature in Kelvin

K1 = Calibration Constant 1

K2 = Calibration Constant 2

The Surface temperature in kelvin was finally converted to surface temperature in degree Celsius (Tc) using the following equation;

$Tc = Tb - 273$ (xii)

F. Relationship between LULC and LST

Monitoring of LST distribution on different LULC will be accomplished by the "combine" tool under "spatial analyst" toolset in ArcGIS 10.3 software to determine the impact of LULC change on LST. Since visible, SWIR and thermal bands used for LULC classification and LST estimation, all the images will be converted to 30m × 30m resolution using standardization approach before performing relationship analysis. The "combine" tool chains multiple raster data sets to generate unique pixel values for every separate combination from the input values. The combine feature supports the combination of given integer pixel values and associated attribute tables. If the value has any decimal point, it is trimmed automatically in the output attribute table, as against other input. The output of the combine tool summarizes the LST distribution in different LULC and outputs the scenario as a table and illustrates them in a different raster. In addition, Pearson's Product Moment correlation will be applied to recognize the impact of the different spatial indicators on surface temperature. The correlation between LST and NDVI; LST and NDWI; and LST and NDBI will be calculated in this study using the scatter plot tool in QGIS 3.8.1 software.

IV. RESULTS AND DISCUSSION

Based on the supervised maximum likelihood classification technique, Landuse landcover (LULC) maps were obtained for the period of three decade and area estimates and change statistics were computed. Figure 3 show the LULC maps for the year 2000, 2010 and 2020 respectively.

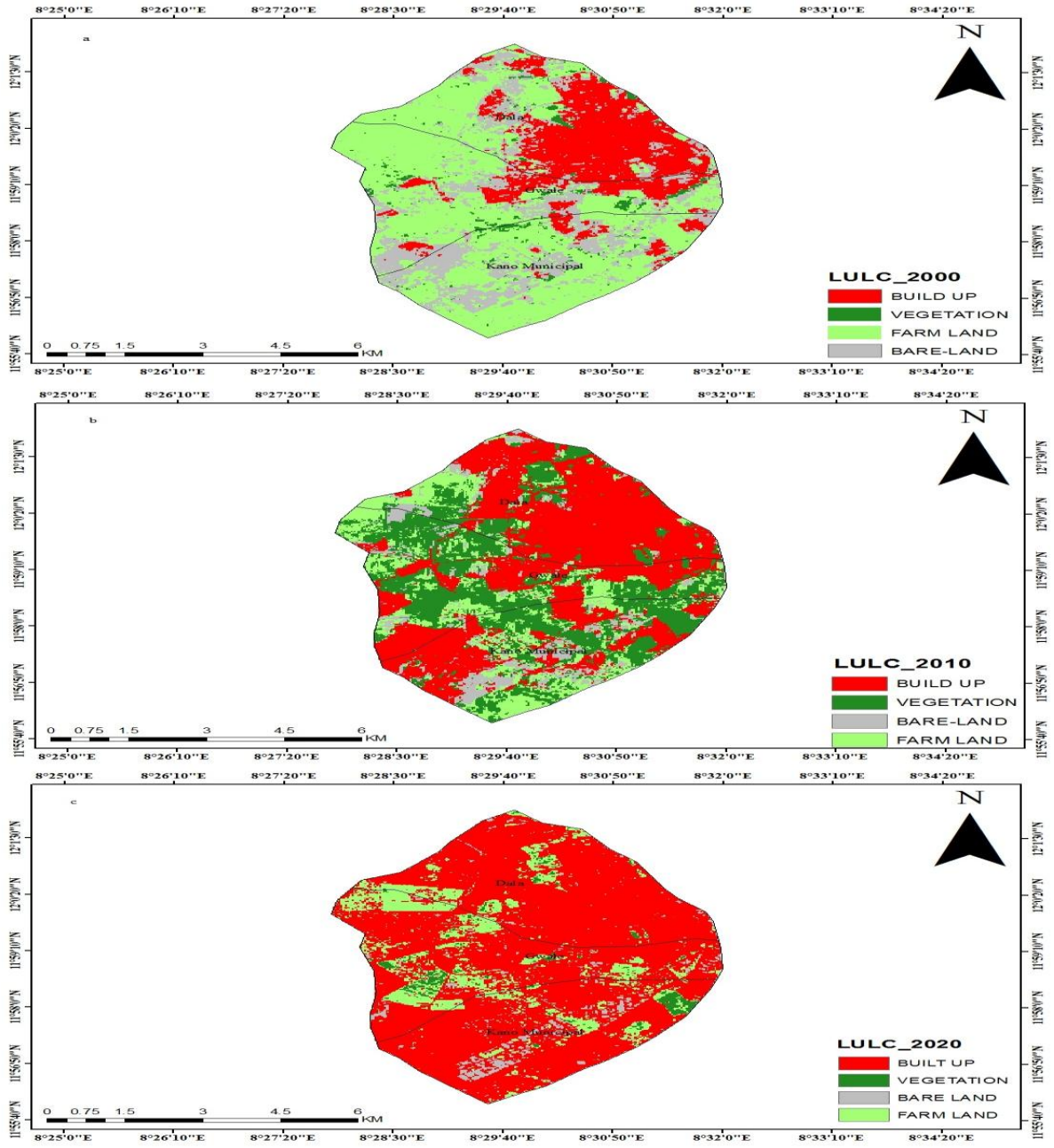

Figure 3: Land use land cover map of study area (a) 2000 (b) 2010 and (c) 2020

Table 2 summarizes the area estimates for the land use land cover classes of the study area derived from the classification results. Among all LULC types, Built- Up Area constituted the predominant type of land cover in all series 2000, 2010 and 2020 occupying 21.40% of the total area in 2000, 45.12% in 2010 and 70.10% in 2020. Farm Land is the second largest land use type covering 30.09% of the total area in 2000, 18.54% in 2010 and 9.58% in 2020. Bare Land follows Farm Land accounting for 27.14% of the total area and Vegetation constitutes the lowest land use covering 21.37% of the total area 2000, 14.37% in 2010, and 8.19% in 2020. Built-Up shows drastic increase in area from 21.40% in 2000 to 70.10% in 2020. The increase in built-up in 2020 is as a result of urbanization compare to 2010 and 2000, and also the decrease in bare land from 2000 to 2020 is also as a result of urbanization and cutting down of trees, decrease in farmland is also as a result of urbanization within kano metropolis.

Table 2: Area statistics of land use land cover classes from 2000 to 2020

LULC	2000		2010		2020	
	Area (Ha)	%	Area (Ha)	%	Area (Ha)	%
Built-Up	1225.240	21.40	2468.396	45.12	4348.537	70.10
Vegetation	148.609	21.37	1606.482	14.37	120.034	8.19
Bare Surface	1377.791	27.14	490.795	21.97	257.177	12.40
Farmland	2718.675	30.09	904.643	18.54	744.568	9.58

Table 3 illustrates the changes in all LULC types from 2000 to 2020. It shows the numerical change in area of all LULC types in terms of hectare and percentage with respect to that of corresponding LULC types in the previous year, whereas Figures 8-10 show the percentage change in area with respect to that of the given year graphically.

During the first period (2000-2010) the land use change is characterized by abrupt rise in Vegetation area by approximately 26.7%. On the other hand, Farm Land decreased by 33.16% Built-Up increased by 22.72% whereas Bare Land decreased by 16.228%.

In the second period (2010-2020), Built-Up increased sharply by approximately 34.37%. Vegetation area showed an opposite trend in this period as compared to the first period with area declining by -27.18%. For Bare Land, the declining trend reduced drastically from -16.22% to 40.73 in this period. Farm Land maintained the same trend as that of the first period.

This period (2000-2020) is in fact the overall change from the first and the second period. There is extreme increment in Built Up area by approximately 57% while Bare Land showed a sharply decline by 24.51%. Vegetation have reduced by 90%, while Farm Land continue on a negative trend from -2.93% in a second period to -36.09% in third period.

A. *Land Surface Temperature*

Figure 4 shows the Land Surface Temperature (LST) maps of the study area in 2000, 2010 and 2020. LST ranged from 13.40^0C to 31.90^0C in 2000, 4.60^0C to 3.119^0C in 2010 and 22.50^0C to 36.80^0C in 2020. The maximum temperature increased by around 7.21^0C during 2000 to 2010 and then declined sharply in the year 2020 by around 2^0C.

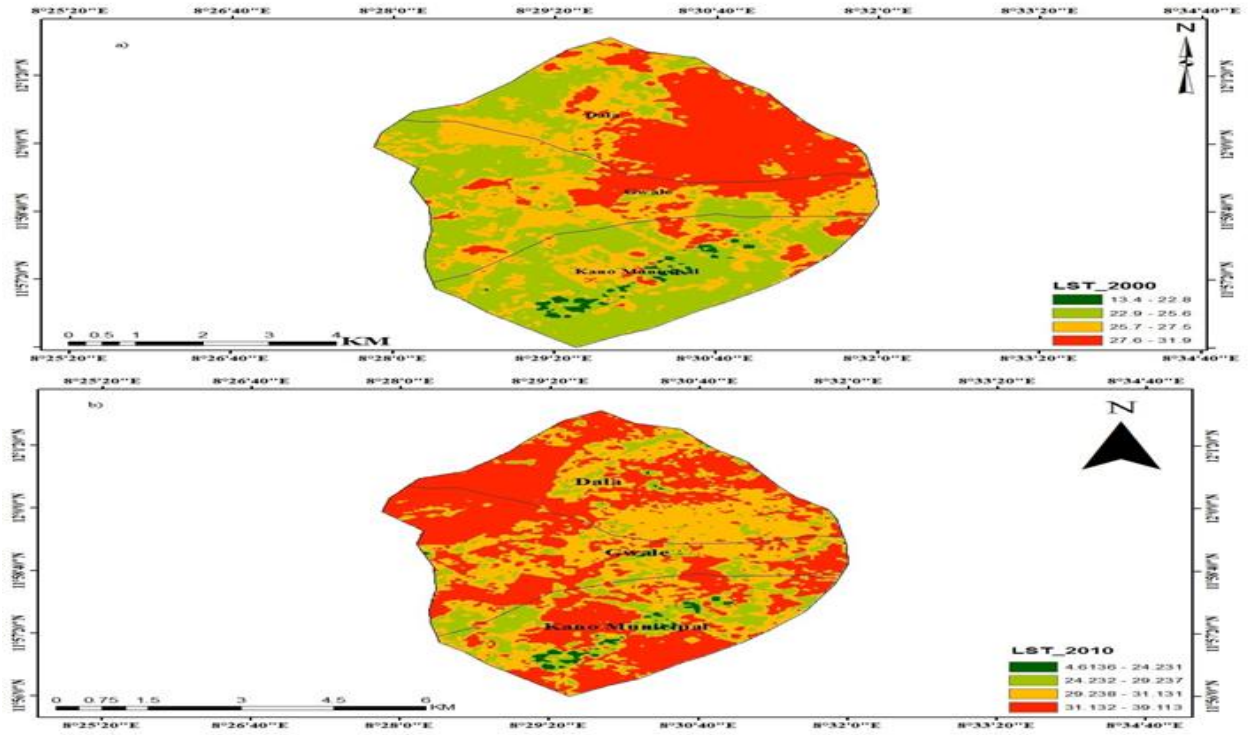

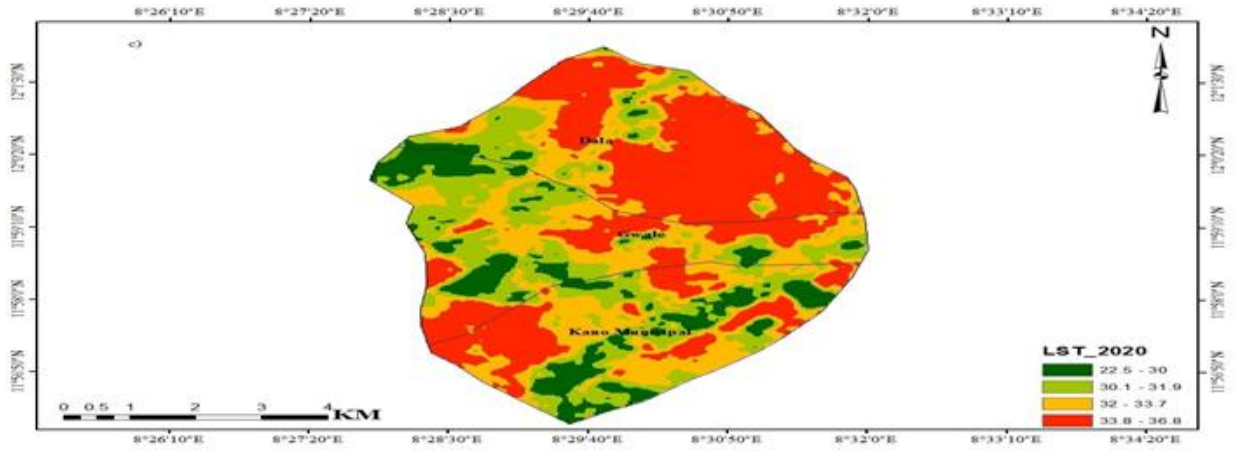

Figure 4: LST of the study area. a) 2000 b) 2010 and c) 2020

B. *Normalized Difference Vegetation Index*

Figure 5 shows the spatial distribution of NDVI in the study area. The area with the highest NDVI values appeared in the edges, which represent the Built-Up area. The area with the lowest NDVI values appeared in dark green color which represents vegetation.

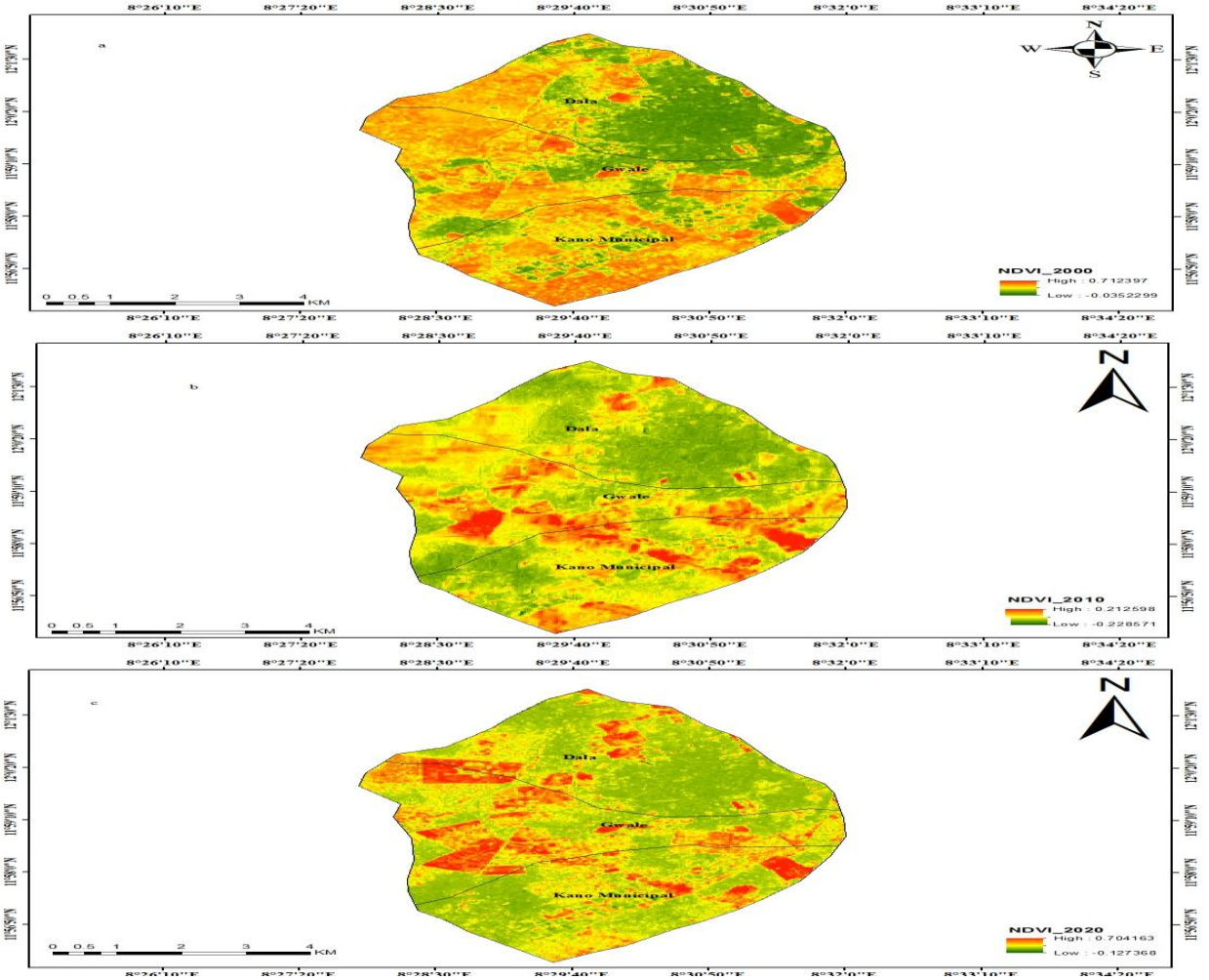

Figure 5: NDVI within each LULC class in a) 2010 b) 2010 c) 2020

C. *Normalized Difference Built-Up Index*

Normalize Difference Built-up Index (NDBI) maps (Figure 6) revealed the same pattern to the NDVI maps in the sense that Built-Up and Bare Land areas with high Normalize Difference vegetation Index (NDVI) values also received high Normalize Difference Built-up Index (NDBI) values. Likewise, Vegetation and Farm Land area with low Normalize Difference vegetation Index (NDVI) received low Normalize Difference Built-up Index (NDBI) value. The lowest NDBI is possessed by Vegetation while the highest value is possessed by Bare Land. In general, built-up areas have higher reflectance in relation to mid-infrared (MIR) band and is thus expected to have higher NDBI but some studies show that reflectance for certain types of vegetation increases as water content decreases ([24] and [25]). The drier vegetation can even have higher reflectance to mid-infrared (MIR) resulting in higher NDBI [25]. Therefore, considering dry vegetation in barren land in higher hills and possibly due to soil characteristics in low land, bare Land areas exhibited higher NDBI values.

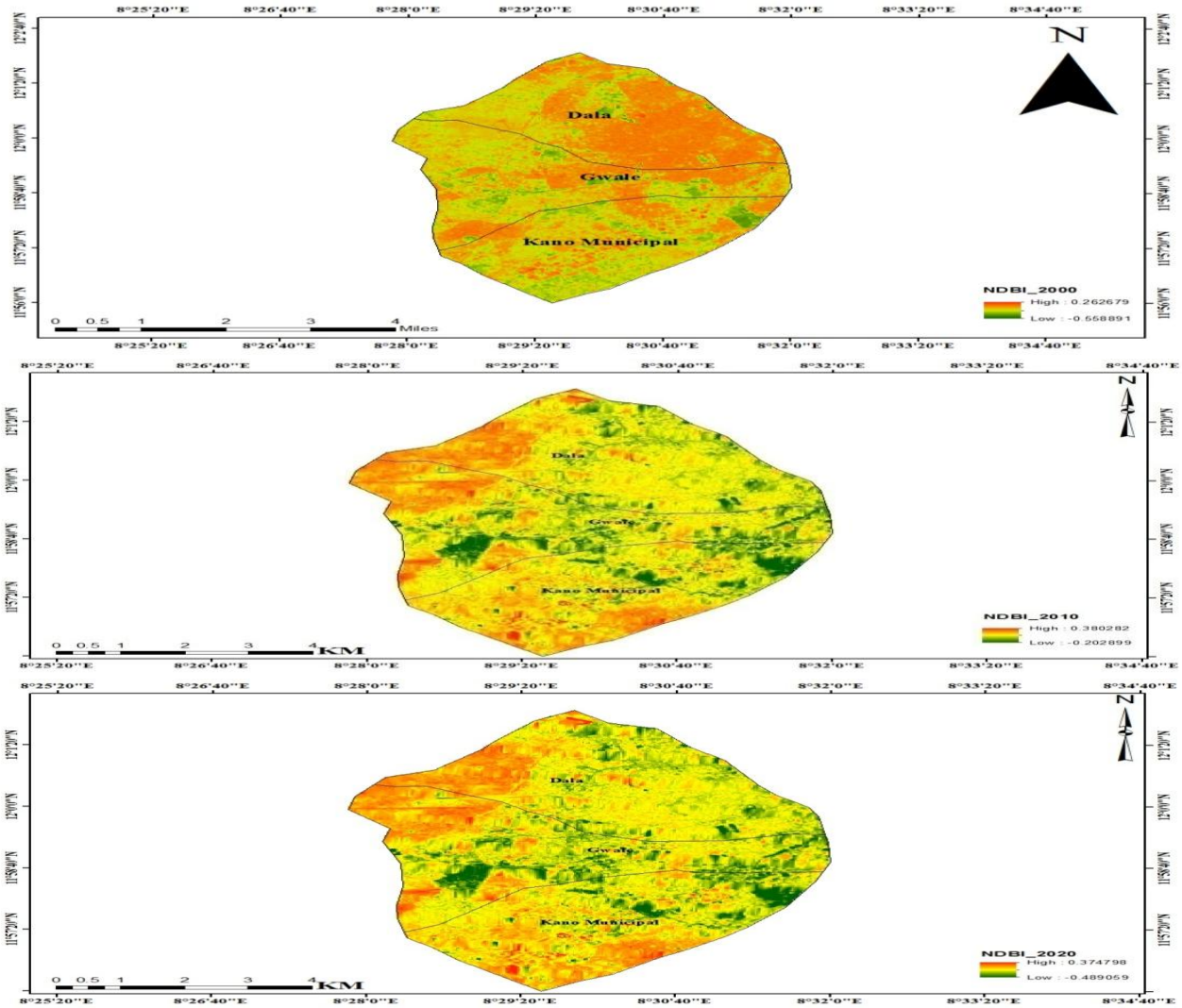

Figure 6: NDBI within each LULC class in 2000, 2010 and 2020

D. *Normalized Difference Water Index*

Figure 7 shows the spatial distribution of Normalize Difference Water Index **(**NDWI) in the study area. Most of the LULC classes received low NDWI value. As expected, water supposed to have highest NDWI value in all the years but my study areas do not have water. Moisture in this case represents water Whereas Vegetation and Farm Land got the lowest NDWI.

Though the mean NDWI value is highly negative, some portion of Built-Up which is shadowed due to relief and consisting of moist showed quite high NDWI value. It can also be observed that the range of NDWI value slightly increases from the year 2000 to 2010 and then sharply decreases in 2020.

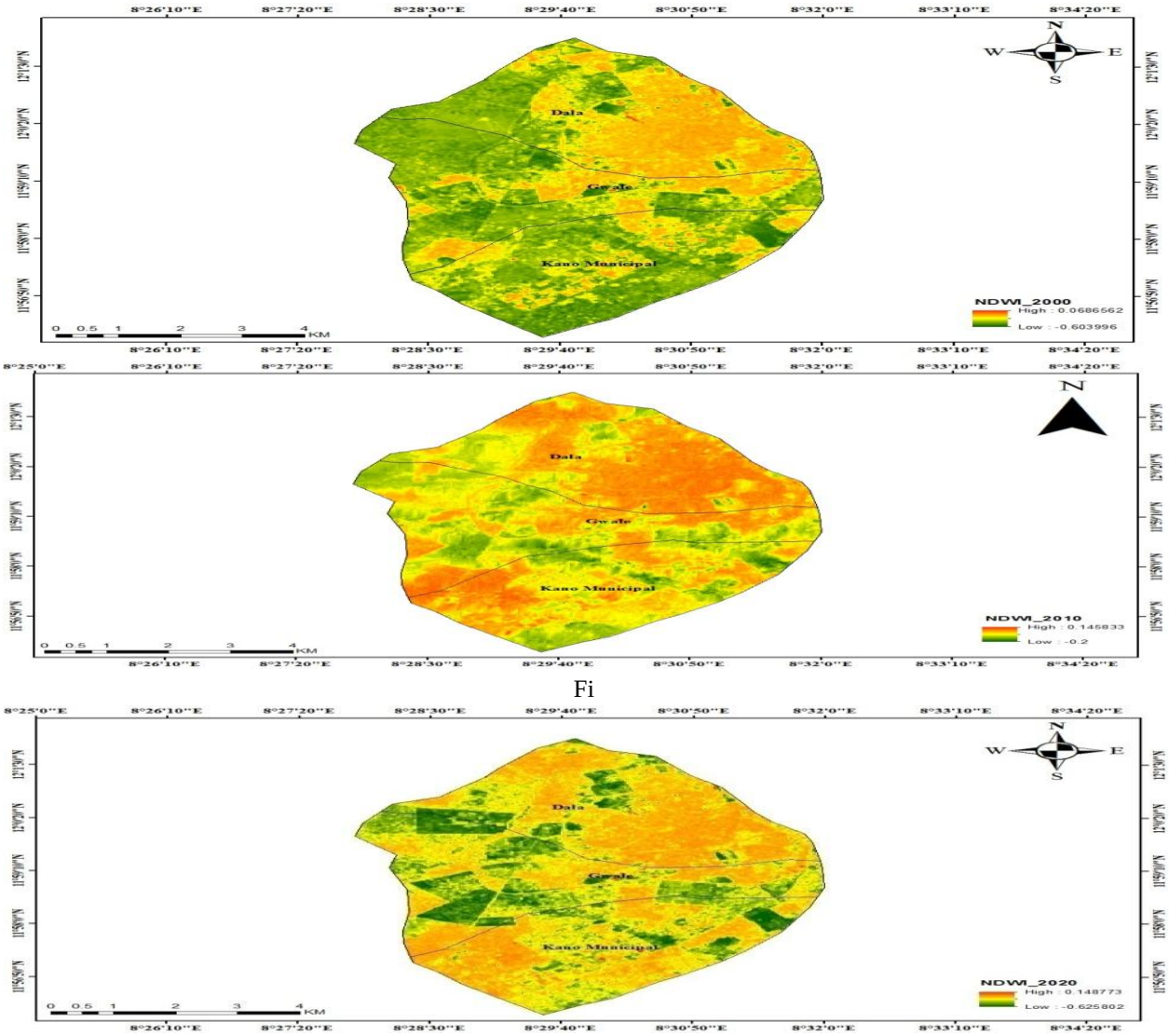

Fi

gure 7: NDWI within each LULC class in 2000, 2010 and 2020

E. *Linear Regression of LST and LULC indices*

To assess the relationship between LST and LULC indices, their correlation was computed. NDVI, NDBI and NDWI were the land use land cover indices used for this purpose. The result shows that the correlation between LST and NDBI is significantly positive whereas the correlations between LST and NDVI, NDWI are significantly negative. Built up area contributes to the increase in the LST while vegetation and Bare Land content have opposite effect. This illustrates the importance of vegetation in the mitigation of UHI effect.

V. CONCLUSIONS

Although the land surface temperature (LST) is widely evaluated in global temperature variation as a result of climate change, the application of integrated soft computing models is still limited to use for detecting LST. This study aimed to design an integrated soft computing model to detect the LST of part of Kano municipal area. Four models were developed and compared, namely LULC, LST, NDVI, NDBI, and NDWI. Landsat images and different software were utilized to mine the LST

changes from 2000 to 2020. In addition, a statistical analysis was conducted to assess the performance of the developed models. From the results, the following can be concluded. First, the comparison of temperature values for the studied periods through image's analyses shows that there has been a significant change in temperature in Dala, Gwale and Kano municipal; the temperature is increased by 0.28°C/year. In addition, the vegetation cover decreased due to the population explosion and economic activities. In addition, the classification of NDVI, NDWI, NDBI, and geographic changes of study area and previous temperature records show that the surface and previous LST changes have a significant impact on the LST prediction of the study area.

REFERENCES

[1] UN (United Nations). (2014). World Urbanization Prospects. Department of Economic and Social Affairs. Retrieved 15 November 2016, from http://esa.un.org/unpd/wup/Highlights/WUP2014-Highlights.pdf

[2] Mohajerani, A. Bakaric, J. and Jeffrey-Bailey, T. 2017, 'The urban heat island effect, its causes, and mitigation, with reference to the thermal properties of asphalt concrete', *Journal of Environmental Management*, Elsevier, United Kingdom, vol. 197, pp. 522-538 ISSN: 0301-4797.

[3] Okereke, P. (2008) Climate Change the Scientific Basis; Adapted from IPCC Working Group I, UNEP Report (2007).

[4] Intergovernmental Panel on Climate Change (IPCC). *Climate Change 2013: The Physical Science Basis, Contribution of Working Group I to the Fifth Assessment Report of the Intergovernmental Panel on Climate Change*; Cambridge University Press: Cambridge, MA, USA, 2013; ISBN 978-1107661820

[5] Uba, M.M. (2015) Location analysis of filling stations in Kano Metropolis, Nigeria. Unpublished Masters Degree Thesis, Ahmadu Bello University, Zaria.

[6] Weng, Q. (2001). Thermal infrared remote sensing for urban climate and environmental studies: Methods, applications, and trends. *ISPRS J. Photogram. Remote Sens*, *64*, 335344.

[7] Shaharuddin, A. (2006). The Effects of urban heat islands on human comfort: A case study of Klang Valley Malaysia. *Global Journal on Advances Pure and Applied Sciences* Vol.2 pp 187-197.

[8] Maiwada AD (2000) Disappearing open spaces in Kano Metropolis. In: Falola JA, Ahmed K, Liman MA, Maiwada A (eds) Issues in land administration and development in Northern Nigeria. Department of Geography, Bayero University, Kano

[9] National Population Commission, (2006). Legal notice on publication of 2006 census final Results. Retrieved May 16, 2012 from http://www.placng.org/legal%notice% 200n%20publication%20of%2006%census20final %20resultpdf

[10] United Nation Development Programme (2004). Annual Report. Research and Documentation Directorate (2009). Kano Urban Planning Development Agency, Kano State Government.

[11] Umar, M.U., Satish, K., (2015). Spatial and Temporal Changes of Urban Heat Island in Kano Metropolis, Nigeria. Journal of Engineering Science and Technology · April 2015.

[12] Adamu, M., Yakudima, I. I., Alhaji, M., Nabegu, A. B., Ado, Y. U., Umar, B. M., *et al* (2014). Overview of the Physical and Human Setting of Kano Region, Nigeria. *Researchjournali's Journal of Geography*, Vol. 1 No. 5.

[13] Kano State Bureau for land Management (2018). Kano Geographic Information Services KANGIS), Kano State Government.

[14] Dankani, I. M. (2013). Affordable Housing provision In Kano North Western Nigeria: The Imperative for the Creation of Sustainable City. International Journal of Management and Social Sciences Research 2 (8), 189-198.

[15] Marafa, I. (1999). Spatial technology for natural risk management. *Disaster Prevention and Management*, vol. 7 (2) 364 – 373.

[16] Naabba, G. (2002). "Challenges of disaster vulnerability reduction in River State, Nigeria", Disaster Prevention and Management: An International Journal, 20 (1)27.

[17] Lillesand, T., Ralph, W.K. & Chipman, J. (2016). Remote Sensing and Image Interpretation (ed. 6). John Wileg & Sons, Inc.

[18] Saha, Y., Nie, J., Li, G., Zhang, C. & Wang, W. (2005). Study on land use and land cover change with the integration of RS, GIS and GPS technologies the case of Baotou City In the ecotone of agriculture-animal husbandry, China. *Geoscience and Remote Sensing Symposium* Presented in IGARSS. 2008 International IEEE, pp. IV.

[19] Chavez, J.R. (1988). The impact of urban areas on weather. Q. J. R. *Meteorol. Soc. 132*, 1–25.

[20] Marino, I., Manevski, K., Kalaitzidis, C. and Edler D. (2011). Comparison between FLAASH and ATCOR atmospheric correction modules on the basis of worldview-2 imagery and in situ spectro radiometric measurements, in: 7th EARSeL Workshop on Imaging Spectroscopy, Edinburgh. Accessed 17Th July 2015 from http://www.earsel2011.com/content/Proceedings/S12_4_Manak os_paper.pdf

[21] Gascon, N., Cirach, M., Dadvand, P., Valentin, A., Nieuwenhrinjsen, M., and Martinez, D.

A. (2016). Normalized difference vegetation index (NDVI) as a marker of surrounding greenness in epidemiological studies: A case of Barcelona. *Journal of Urban Forestry and Urban Greenning , 19*, 88-94.

[22] Abutaleb k, A Ngie, A Darwish, M Ahmed, S Arafat, F Ahmed (2015) Assessment of urban

A. heat island using remotely sensed imagery over creater cairo, Egypt.

[23] Arekhi, M., Goksel, C., and Sanli, F. a. (2019). Comparative Evaluation of the Spectral and

A. Spatial Consistency of Sentinel-2 and Landsat-8 OLI Data for Igneada Longos Forest. *International Journal of Geo-information , 8* (56), 56.

[24] Cibula, W.G., Zetka, E.F. & Rickman, D.L. (2016). Response of thematic mapper bands to plant water stress. *International Journal of Remote Sensing*, 13, 1869-1880.

[25] Gao, B.C. (2010). NDWI–A normalized difference water index for remote sensing of vegetation liquid water from space, Remote Sensing of Environment, 58(3), 257–266.